ISSN: 0975-8585

Research Journal of Pharmaceutical, Biological and Chemical Sciences

Molecular Docking, ADME, and Molecular Dynamics simulation Studies of Quinazolinone- Cinnamaldehyde Schiff Base derivatives.

Abbas H Abdulsada[1]*, Baneen M Obaid[1], Aseel A Obieed[2], Saja H Hashim[1], Tabark E Jassim[2], Hind Z Turki[3], and Hajar J Khazaal[4].

[1]Department of Pharmaceutical Chemistry, College of Pharmacy, University of Babylon, Babylon, Iraq.
[2]Department of Pharmaceutics, College of Pharmacy, University of Babylon, Babylon, Iraq.
[3]Department of Pharmacology and Toxicology, College of Pharmacy, Babylon, Iraq.
[4]Department of Pharmacognosy and Medicinal Plants, College of Pharmacy, University of Babylon, Babylon, Iraq.

ABSTRACT

Two novel Schiff bases derived from Quinazolinone and Cinnamaldehyde have been appraised for their potential usefulness against several bacterial pathogens. Molecular docking was implemented using the crystalline structure of eight potential bacterial targets, wherein the two compounds the binding affinity of them was determined by docking with the target binding site. Computer predictions were made using MOE 2024.06, and both ligands were drawn using ChemDraw version 22.0.0. In silico ADME prediction studies unveiled the remarkable prospects for receptor interaction, and the drug-likeness properties was estimated utilizing the Swiss ADME website. Furthermore, Molecular Dynamics simulations of ligand 4a docked at the active site of 3LN1 (Cyclooxygenase-2) were executed using Schrodinger Suite 2024-3 software for 50 ns, computing RMSD, RMSF, Ligand-Protein Contacts, and Ligand Torsion Profile results. Findings indicate the most effective binding energy within the receptor pocket that demonstrates potential activity against the DNA gyrase protein receptor. The greatest binding affinities were elicited by compounds 4a for E. coli DNA gyrase, Human cannabinoid receptors CB2 (-8.54 and -8.00 respectively), both compounds were found to obey Lipinski's rule of five, with superior absorption from the alimentary tract, and both cannot penetrate the blood-brain barrier. Molecular dynamics simulations indicate a Mean Protein RMSD of 2.4 Å, a ligand RMSD of 1.6 Å, and the RMSF analysis shows that the protein residues that interact with the ligand stay within a distance of under 1 Å.

Keywords: Molecular Docking, ADME, Quinazolinone, Cinnamaldehyde

https://doi.org/10.33887/rjpbcs/2025.16.4.9

Corresponding author

ISSN: 0975-8585

INTRODUCTION

Antimicrobial chemotherapy was pivotal in the treatment of human infections. Since the advent of penicillin in the 1920s, there have been numerous antimicrobial agents that have been created or synthesized to manage human infectious diseases, and various such drugs are used in clinics nowadays. Nonetheless, the sheer plurality of these agents and the unending evolution of such methods pose difficulties for clinicians to remain [1, 2]. Increased drug resistance threatens the very effectiveness of these essential medical interventions. Therefore, there has been a growing need for the progress and discovery of novel antibacterial substances with unique targets and a new molecular structure that may help to mitigate the development of cross-resistance [3]. Antimicrobial resistance has been recognized for over 50 years as one of the significant contributors to increased morbidity, mortality, and healthcare costs *+7 [4]. The prevalence of antimicrobial resistance is manifested through three main mechanisms: (i) natural mutations in endogenous cellular genes, (ii) horizontal acquisition of resistance genes by mobilization from exogenous sources, and (iii) further mutations within already acquired resistant genes. These avenues collectively contribute to the adaptability and survival of microorganisms that are otherwise agents of disease against antimicrobial therapy [5, 6]. As a matter of fact, quinazoline and quinazolinone frameworks have gained much consideration in a couple of years back because of their immense therapeutic potential. These structures have been found very effective for some reason, especially as hybrid compounds, to exert antibacterial influence by diversified mechanisms. These hybrids, besides being versatile, place themselves as scaffolds that are useful for designing and discovering new antibacterial agents. The ability of these hybrids to interact multifariously with more than one bacterial target shines them as hopeful candidates against drug-resistant pathogens and shines a door of light towards the discovery of new and innovative antimicrobial treatments [7, 8]. Another study indicates the potential of 4(3H)-quinazolinone derivatives as promising antibacterial agents. These compounds have exerted remarkable antibacterial effects and thus can be considered for further investigation as potential novel anti-infective chemotherapeutics. The action principle of these compounds is directed at bacterial enzyme inhibition and perturbation of some important cellular processes. More precisely, the quinazolinone derivatives are aimed at bacterial DNA synthesis and protein constructs. As a result, normally, there would be an arrest in bacterial proliferation with time due to a general growth delay. These might work on multiple bacterial pathogens and therefore be a possible alternative in the battle against antimicrobial resistance [9, 10].

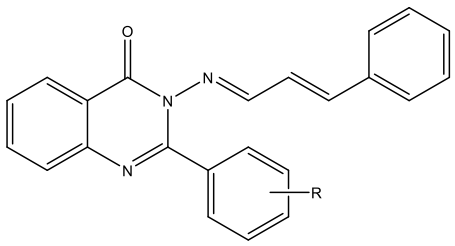

Fig (1): Schiff base derivatives derived from quinazolinone and cinnamaldehyde where Compound 4a: R = 4-CH_3, Compound 4b: R = 2-OH

The synthesis and biological evaluation of novel Schiff base derivatives from quinazolinone and cinnamaldehyde fig (1). Schiff Base 4a and 4b were synthesized by reacting cinnamaldehyde with p-Me or o-OH-phenyl quinazolinone derivatives, respectively. The representation of the imine (C=N) group in the quinazolinone or cinnamaldehyde backbones and the amine characteristic of both Schiff bases. The compounds were obtained in good yields and characterized by IR and 1H NMR. The in silico biological prediction indicated that some of the synthesized Schiff base derivatives are very effective as antimicrobial, anticancer, and anti-inflammation agents, signifying their potential for becoming new drugs [11]. Molecular docking, along with MD simulation, needs to be performed to predict the binding modes of these Schiff base derivatives to bacterial enzymes or receptors, providing valuable insights into the interaction at the molecular level. These computational techniques help in identifying the most effective structural features that contribute to antibacterial activity, offering a pathway for the rational design of more potent antimicrobial agents [12].

Computational method

The proposed Schiff base derivatives were based on insights from a previous study [11], illustrated in Fig (1). To assess the antibacterial effect of these compounds, an in silico molecular ducking (MOE) was

conducted to evaluate their interaction with seven bacterial proteins (2W9S, 4DFR, 3G7E, 5EQG, 6KPF, 3LN1, 7PTG). The crystal structures of macromolecular proteins were protonated using the Amber99 force field. ADME (absorption, distribution, metabolism, and excretion) properties were predicted using the Swiss ADME server to ensure drug-likeness and pharmacokinetic compatibility of the compounds. To get insights into their molecular behavior, Desmond-v7.9 was utilized to implement Molecular Dynamics simulations. Simulations were run for 50 ns under physiological conditions, during which binding mechanisms and conformational changes in the ligand-protein complexes could be analyzed. Computations were based on the structure of the seven proteins (4DFR, 3G7E, 5EQG, 6KPF, 3LN1, 7PTG, 2W9S). It includes the discovery and optimization of potent and selective compounds for pharmaceutical use based on the three-dimensional structure of biological target molecules using docking algorithms. The same has been attributed to several fragment instances other than the actual phrases matching [13, 14].

Preparation of ligands

The ligands discussed in this research were sourced from existing literature. Both molecular structures were recreated using ChemBioDraw Ultra 22.0.0, and subsequently, the ligands were saved in mol format to facilitate their opening in MOE after preparing their molecular structures. These structures were then protonated in 3D at a temperature of 300 ˚C and a pH of 7, followed by energy minimization in MOE using the default parameters. The MMFF94x force field was applied without considering periodicity, while rigid water molecules were subjected to constraints.

Preparation of proteins

The protein crystal structures were sourced from the Research Collaboratory for Structural Bioinformatics (RCSB) Protein Data Bank (PDB) at http://www.rcsb.org/pdb/home/home.do. All crystallographic water molecules were eliminated, except for those that were part of the ligand-protein interactions serving as water bridges. Using the MOE software with its default settings, the protein structure was protonated in three dimensions, and energy minimization was performed. For the molecular docking process, the receptors and solvent atoms were processed, and polar hydrogens were added. During the docking procedure, the ligand atom was specified, and rescoring1 was configured to London dG while rescoring2 was set to GBVI/WSA dG, with the interaction between the ligand and the protein being evaluated.

In silico drug-likeness and ADMET prediction

Target Schiff bases 4a and 4b's physicochemical characteristics and drug-likeness were assessed using the SwissADME website http://www.swissadme.ch/index.php [15]. However, the Molsoft LLC website, https://www.molsoft.com/mprop/, was used to generate the drug-likeness ratings [16].

Molecular Dynamics Simulation

Molecular dynamics (MD) simulations, an improved method for studying macromolecular ligand-receptor interactions, provide dynamic insight beyond the static nature of molecular docking, compound 4a was selected for MD simulations based on docking results. The system was carried out using the SPC liquid sample in a 10 Å box with an OPLS4 charge neutralized with 0.15 M NaCl at neutral PH. Simulations were run for 50 nanoseconds at 300 kV to investigate bond dynamics and stability.

RESULTS AND DISCUSSION

The goal is to create effective substances that show selectivity and possess ideal ADME (absorption, distribution, metabolism and excretion) characteristics.

Molecular Docking

The molecular docking outcomes table (1) highlights that 4b compound shows better binding affinities than 4a in the majority of bacterial protein targets, making it more useful antibacterial agent than 4a, with binding energies attaining up to -7.75 kcal/mol in opposition to Staphylococcus aureus DHFR (2W9S) facilitated by means of multiple hydrogen bonding interactions with GLN(19,95), ILE14, GLY94 and numerous Hydrophobic contacts with ILE(5,31,50), ALA7, GLY15, LEU20, PHE92, fig 2 (A). For

ISSN: 0975-8585

instance, 4b demonstrates superior binding affinity with the 6KPF protein (-8.00 kcal/mol) fig (2 B) due to hydrogen bonding with SER285 and interactions with more than one hydrophobic residue along with PHE(87,91,106,183), HIS95, ILE110, VAL113, and ALA282. While 4a exhibits superior binding affinities for COX-2 (3LN1) and human glucose transporter GLUT1 (5EQG) rendering it a candidate ligand for conditions like pain, obesity, dyslipidemias, and diabetes. These outcomes advocate that the hydroxyl group in 4b enhances its interplay profile, mainly through hydrogen bonding and hydrophobic contacts, in comparison to the methyl group in 4a. The findings underscore 4b compound's capacity as a promising lead compound for further drug improvement research. (17-19)

Table 1: Molecular docking results using MOE software

proteins	ligands	Binding energy (K cal/mol)	Refined RMSD	H-bonding	Hydrophobic interactions
2W9S	4a	-7.71	1.53	GLN19	ILE(5,14,31,50), LEU(20,28,54), PHE92
	4b	-7.75	1.30	GLN(19,95), ILE14, GLY94	ILE(5,31,50), ALA7, GLY15, LEU20, PHE92
3G7E	4a	-8.54	1.78	HOH408	VAL(43,120,167), ILE(78,94), HIS116, LYS103, GLU50, ARG76, PRO79, MET95
	4b	-7.85	1.87	HOH408, PHE104, LYS103	ASN46, ILE(78,94), GLU50, ARG76, PRO79
3LN1	4a	-7.76	0.99	ARG106	TYR(341,371), TRP373, ALA(502,513), VAL(102,335,509), LEU517
	4b	-6.93	1.46	ALA513, VAL509	ARG499, LEU517, VAL335, GLY512, ALA502
4DFR	4a	-6.98	1.70	MET20	ALA7, ASP27, TRP22, LEU28, HIS45
	4b	-7.14	1.71	MET20, ASP27	ALA7, MET20, TRP22, LEU28
5EQG	4a	-7.29	1.11	-	HIS160, ILE164, TRP(388,412)
	4b	-7.06	1.16	THR137, HIS160, ASN288, GLY408	PHE26, TRP388
6KPF	4a	-7.48	1.63	-	PHE(94,183,281), HIS95, LYS109, ILE110, PRO184, ALA282
	4b	-8.00	1.34	SER285	PHE(87,91,106,183), HIS95, ILE110, VAL113, ALA282
7PTG	4a	-7.03	1.55	HOH412	ASN48, SER49, ARG78, ILE(80,96), PRO81
	4b	-7.13	1.63	HOH412	ASP51, ARG78, ILE80, PRO81, VAL122

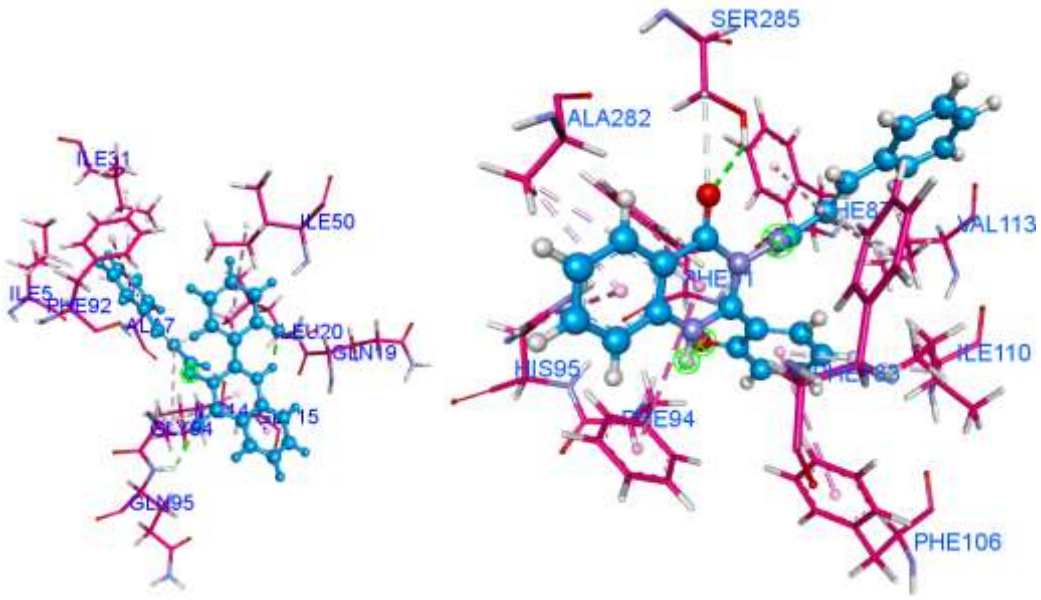

A B

Figure 2: 4b compound interaction (A): with 2W9S and (B): with 6KPF

ADME

The preference of contemporary drugs and designing their proper formulation type are principally conditional on the physicochemical properties, which comprise the hydrogen-bonding capability, solubility, molecular weight (MW), topological polar surface area (TPSA), and molar refractivity (MR); therefore, the physicochemical properties (Table 3) are the essential aspects for synthesizing new drug candidates and should oriented with drug-likeness rules like Lipinski's rule, Muegge's rules, Ghose's filter, Veber's filter, Pfizer rule for CNS activity, Egan's filter and lead-like rule which are critical during the early stages of drug discovery process enabling the assessment whether the compound under study is acceptable as drug-like molecule. According to these guidelines, we determined that both Schiff bases (4a and 4b) adhere to the four drug-likeness principles (Lipinski, Ghose, Veber, and Egan rules), and these derivatives meet the criteria for potential new drug candidates (16).

Table 2: The physicochemical properties, drug-likeness, and drug-likeness scores of 4a and 4b compounds

properties	compound 4a	compound 4b
Formula	C24H19N3O	$C_{23}H_{17}N_3O_2$
Molecular weight (MW) g/mol	365.43	367.40
Heavy atoms NO	28	28
Aromatic heavy atoms NO	22	22
Fraction Csp^3	0.04	0.00
Rotatable bonds NO	4	4
H-bond acceptors NO	3	4
H-bond donors NO	0	1
Molar refractivity	115.77	112.83
TPSA	47.25	67.48
***M* log P (solubility)**	5.08	4.04
***W* log P (solubility)**	4.81	4.21
***X* log P (solubility)**	4.96	4.24
Lipinski filter violations	1: MLOGP>4.15	0
Ghose filter violations	0	0
Veber (GSK) filter violations	0	0
Egan (pharmacia) filter violations	0	0
Drug-likeness model score	0.47	0.36

The analysis of drug-likeness model scores hinges on the positive and negative readings assigned to the target compounds, indicating that a compound is classified as drug-like when it has a positive drug-likeness score. Conversely, a compound is deemed nondrug-like if its drug-likeness score is negative (20). Based on this standard, we realize that the two Schiff bases (4a and 4b) demonstrates drug-likeness scores equal to 0.47 and 0.36, respectively, and are thus regarded as drug-like.

ISSN: 0975-8585

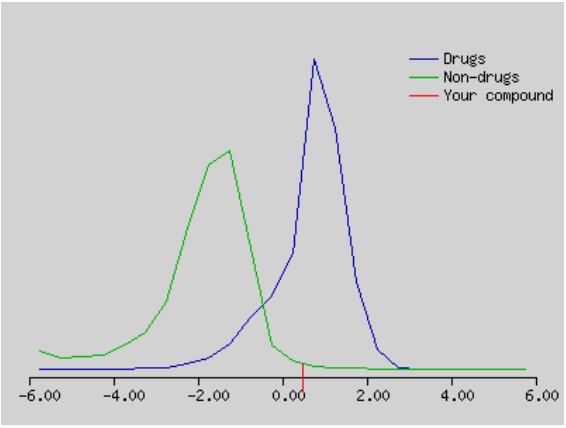

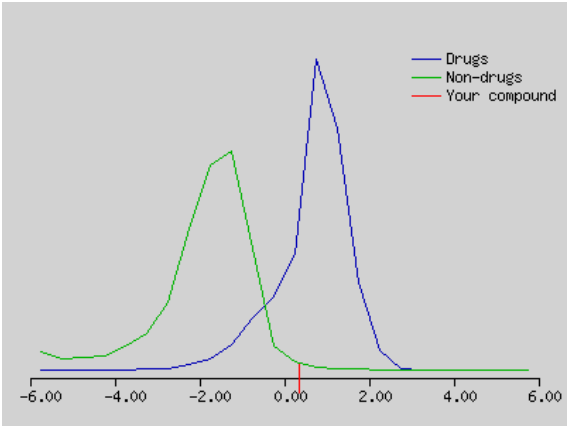

Figure 3: Drug-likeness model score (4a): 0.47 Figure 4: Drug-likeness model score (4b): 0.36

Table 3: Toxicity and metabolism prediction analysis

Properties	4a	4b
Toxicity		
Human hepatotoxicity (H-HT)	0.73	0.566
Carcinogenicity	0.845	0.854
AMES Toxicity	0.868	0.859
Skin sensitization (SS)	0.565	0.565
Eye irritation (EI)	0.841	0.889
Eye corrosion (EC)	0.003	0.003
Metabolism		
CYP1A2 inhibitor	Yes	Yes
CYP2C19 inhibitor	Yes	Yes
CYP2C9 inhibitor	Yes	Yes
CYP2D6 inhibitor	No	No
CYP3A4 inhibitor	Yes	Yes

Assessing human hepatotoxicity (H-HT) is crucial for evaluating the risks associated with new pharmaceuticals. Liver damage and injury resulting from a drug's effects pose significant safety issues for patients, potentially predisposing to the drug's discontinuation from the market (21). The newly targeted chemical entities are classified as either non-hepatotoxic, or H-HT negative, with a score ranging from 0 to 0.3, or hepatotoxic, or H-HT positive, which is further divided into two categories: moderate toxic potential with a modeled score between 0.3 and 0.7 and high toxicity with a score from 0.7 to 1.0. Both Schiff bases (4a and 4b) were anticipated to be hepatotoxic (H-HT positive) with intense and moderate toxicity respectively. Carcinogenic materials generally elevate the risk of cancer due to metabolic cells destruction besides DNA damage which is at once correlated with many biological processes in the body (22). Compounds are categorized as non-carcinogenic with a predicted value ranging from zero to 0.3, moderately carcinogenic with values from 0.3 to 0.7, or strongly carcinogenic with predicted values between 0.7 and 1.0. Hence, both compounds are described as potential carcinogens and revealed high predicted values. The compounds mutagenicity were tested by Ames test .The target compound is considered either non-mutagenic (predicted value of 0 to 0.3) or mutagenic with strong mutagenicity (predicted value of 0.7 to 1.0) and medium mutagenicity (predicted value of 0.3 to 0.7). based on these rules both compounds are highly mutagenic (23). Concerning Eye corrosion , Eye irritation and Skin sensitization; Compounds are predicted to be safe (predicted value of 0 to 0.3), moderately harmful (predicted value of 0.3 to 0.7) or strongly detrimental (predicted value of 0.7 to 1.0). both compounds are expected to cause moderate Skin sensitization, highly eye irritant and with no meaningful Eye corrosion effect. Table (4) denote that four enzymes (specifically: CYP1A2, CYP2C19, CYP2C9, and CYP3A4)are

inhibited by both compound . Additionally, both Schiff bases 4a and 4b were anticipated not to inhibit the CYP2D6 enzyme.

Table 4: The absorption and distribution properties prediction

Properties	4a	4b
Absorption		
Caco-2 permeability (log cm s^{-1})	-4.862	-4.911
MDCK permeability (cm s^{-1})	1.4×10^{-5}	1.5×10^{-5}
P-glycoprotein-inhibitor	0.999	0.18
P-glycoprotein-substrate	0.002	0.001
Distribution		
Plasma protein binding (PPB, %)	99.64	99.57
Fraction unbound in plasma (FU, %)	0.785	0.778
Volume distribution (VD, L kg^{-1})	0.245	0.207

To reach systemic circulation a drug molecule must partition through barriers like GI mucosal cell and blood vessels membranes. To appraise drug membrane permeability, we exploited the adenocarcinoma cell lines (Caco-2) of the human colon . In consequence, Caco-2 cell absorption permeability has been a consequential measure for the newly developed a drug molecule (24). A lead compound is considered suitable for Caco-2 permeability when its modeled value is > −5.15 log cm s−1. According to the rule of Caco-2 permeability, we found that both Schiff base compounds (4a and 4b) possess suitable Caco-2 permeability with values of -4.862 and -4.911 log cm s−1 respectively. The apparent permeability coefficient (Papp) serves as a measure for assessing how effectively target compounds are membrane-permeable in the body. This necessitated the creation of Madin–Darby Canine Kidney cells (MDCK) for use as a model in permeability testing. Additionally, we utilized the Papp values obtained from MDCK cell lines to investigate the impact of the blood–brain barrier (BBB), (25). The lead compound is regarded to be of high passive MDCK permeability when its Papp is more than 20 × 10−6 cm s−1. Table 5 demonstrate that the target compounds 4a and 4b have a high passive MDCK permeability of more than 20 × 10−6 cm s−1 with Papp values of 1.4 × 10−5 to 1.5 × 10−5 cm s−1 respectively.

P-glycoprotein is a membrane protein that is encoded by the ABCB1 gene in humans. Its main role is to act as a drug transport protein, which is essential for controlling the distribution and availability of different medications. Thus, a known inhibitor or substrate may enhance cellular absorption and aid in predicting the pharmacokinetics of drugs (26). A target compound is classified as an effective P-glycoprotein inhibitor or substrate with a expected value ranging from zero to 0.3: excellent; from 0.3 to 0.7: medium; and from 0.7 to 1.0: poor. Accordingly, 4a is a non-inhibitor for P-glycoprotein with values of 0.999, while 4b is considered an inhibitor with a predicted value of 0.18. Both compounds are P-glycoprotein substrates with expected values a range 0.002 and 0.001.

The pharmacodynamic characteristics of the medications are influenced by their binding to plasma proteins (PPB) and the proportion of free drugs in the plasma (FU). Plasma protein binding (PPB) pertains to the reversible association between drugs and proteins found in blood plasma. This interaction establishes a reservoir of the drug, but merely the unbound (free) drug is capable of exerting therapeutic effects (27, 28). A lead compound is deemed to have appropriate plasma protein binding when its predicted plasma protein binding (PPB) value is below 90% and its predicted unbound fraction (FU) value is at least 5%. Conversely, medications that exhibit high plasma protein binding of over 90% and have a expected value for FU lower than 5% might possess a narrow therapeutic index and reduced efficacy in crossing cellular membranes. Both Schiff bases (4a and 4b) demonstrate a strong affinity for plasma proteins, with anticipated binding values exceeding 90% (in fact, over 99%). Additionally, the predicted free fractions (FU) for these compounds are below 5% (0.785% and 0.778%), suggesting that they might possess a low therapeutic index and exhibit limited effectiveness in traversing membranes. The volume of distribution (Vd) is a pharmacokinetic measurement that reflects the degree to which a drug disperses throughout body

tissues relative to the plasma. It is characterized as the quotient of the systemic drug load in the body and the concentration of that drug in the plasma. An increased Vd indicates that a drug is more thoroughly distributed in the tissues than it is retained within the bloodstream. If the anticipated volume distribution of the target compound falls between 0.04 and 20 L kg−1, it indicates that the compound exhibits a favorable volume distribution (29). The two target Schiff bases, 4a and 4b, demonstrate appropriate volume distributions of 0.245 and 0.207 L kg−1, respectively.

Molecular Dynamic Simulation

The 3LN1 (Cyclooxygenase-2) protein, selected depending upon the results of docking at same time, it is a a key mediator of inflammatory pathways and its increased expression has likewise been reported in multiple human cancer types. It represents a key enzymatic protein worried in biological pathway, making it a prime target for designing inhibitors (30). Molecular dynamics (MD) simulation turned into accomplished to evaluate the binding balance and interplay profile of the 4a compound with 3LN1 protein. Simulation parameters blanketed an NPT ensemble at 300 K for 50 ns.

The RMSD

The Root Mean Square Deviation (RMSD) of the protein-ligand complex turned into calculated to evaluate the overall system balance. The RMSD values of the ligand and protein stabilized after the preliminary equilibration phase (~10 ns), suggesting that the device reached a regular state. This displays minimal conformational changes inside the protein-ligand complex at some stage in the simulation, indicative of stable binding.

Protein RMSD

The protein's RMSD values remained in the suitable range (1-3 Å), confirming the structural stability of the protein throughout the MD simulation. These values advise that the protein's conformational flexibility did not exceed standard thermal fluctuations, ensuring the binding site maintained its geometry fig (5).

Ligand RMSD

The ligand RMSD, measured relative to the protein backbone, stabilized at 1.6 Å, demonstrating its constant positioning inside the binding pocket. This implies that the ligand 4a did no longer show off vast glide and maintained favorable interactions with the 3LN1 protein fig (5).

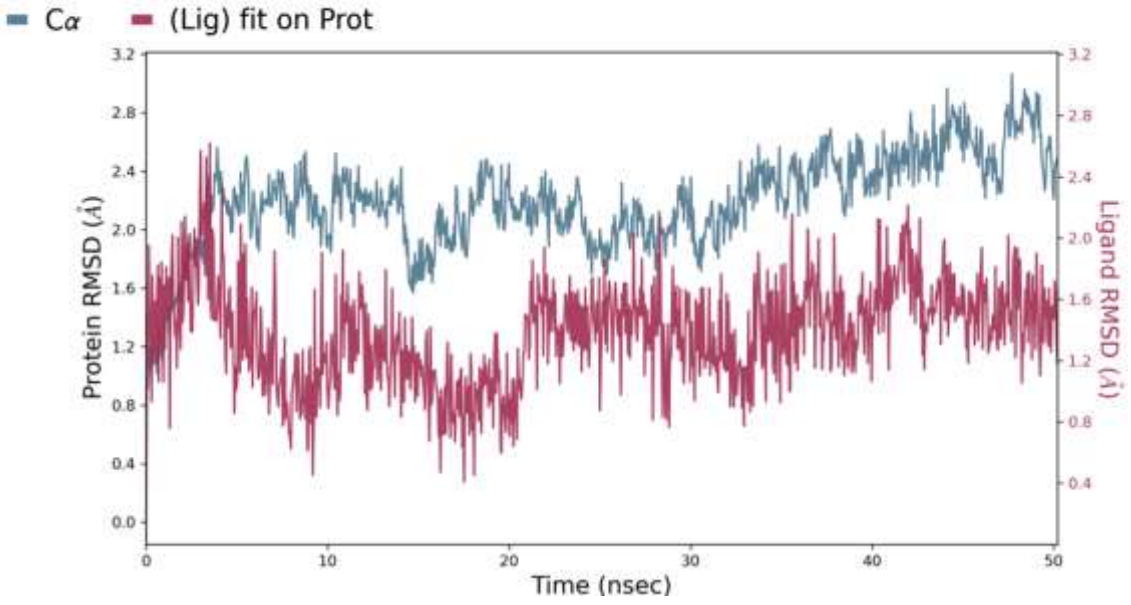

Figure 5: RMSD of the atoms of protein and the ligand over time

ISSN: 0975-8585

Protein RMSF

The Root Mean Square Fluctuation (RMSF) of protein residues indicated better flexibility in loop areas and terminal ends, as predicted. However, residues worried in ligand binding showed minimum fluctuations, confirming their role in strong interactions with the 4b compound fig (6).

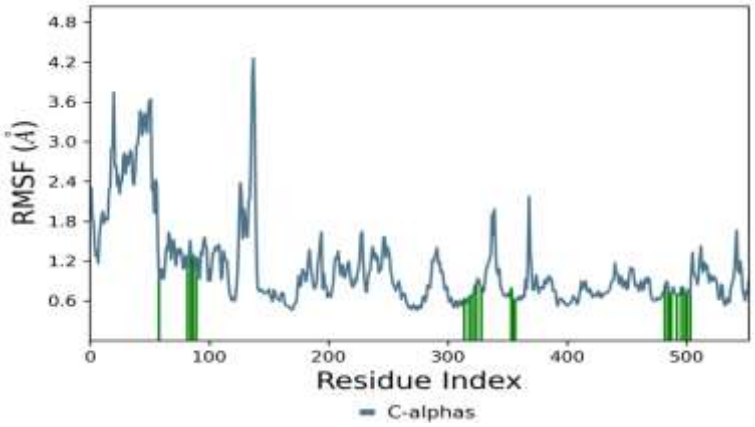

Figure 6: RMSF of protein

Ligand RMSF

The RMSF values for compound 4a's atoms remained low in the course of the simulation, suggesting a strong binding conformation within the protein's active site. This stability is indicative of strong protein-ligand interactions, which might be critical for the compound's inhibitory activity fig (7).

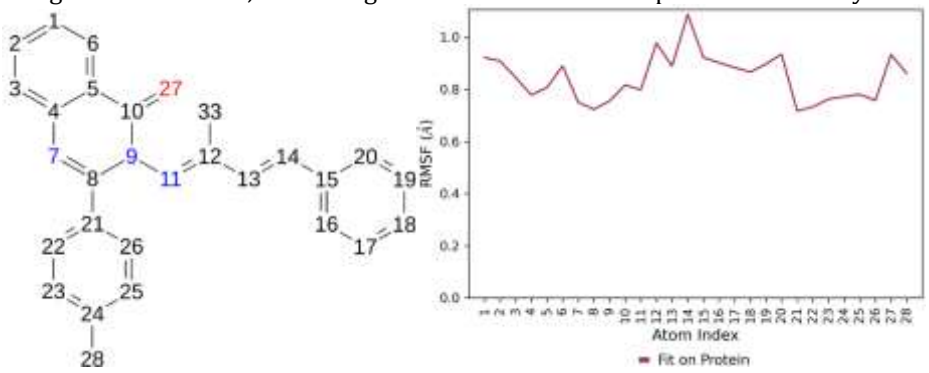

Figure 7: ligand RMSF

Ligand-Protein Contacts

Ligand RMSF analysis discovered constrained atomic fluctuations, mainly for atoms worried in essential hydrogen bonding and hydrophobic interactions. This shows that the ligand continues an inflexible conformation whilst bound, reducing entropic consequences all through binding.

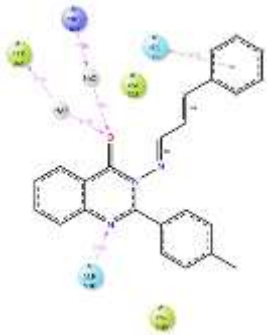

Figure 8: Ligand- Protein Contacts

ISSN: 0975-8585

Protein-Ligand Contacts (cont.)

The protein-ligand touch evaluation discovered a couple of hydrogen bonds, hydrophobic interactions, and water bridges, with a few interactions persisting for over 70% of the simulation time. Key residues, including [TYR341, ARG106, HIS75, SER516, VAL509], played pivotal roles in anchoring the ligand in the binding web page.

Protein-Ligand Contacts

Hydrogen bonds, π-π stacking interactions, and water-mediated interactions contributed notably to the ligand's binding affinity. The staying power of these interactions over the simulation underscores the ligand's potential as a robust inhibitor.

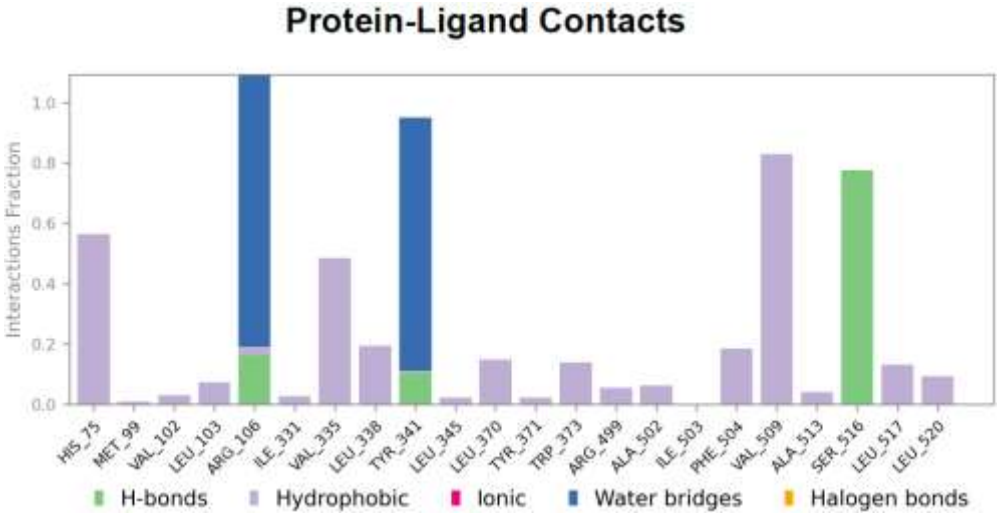

Figure 9: Protein-ligand contact histogram

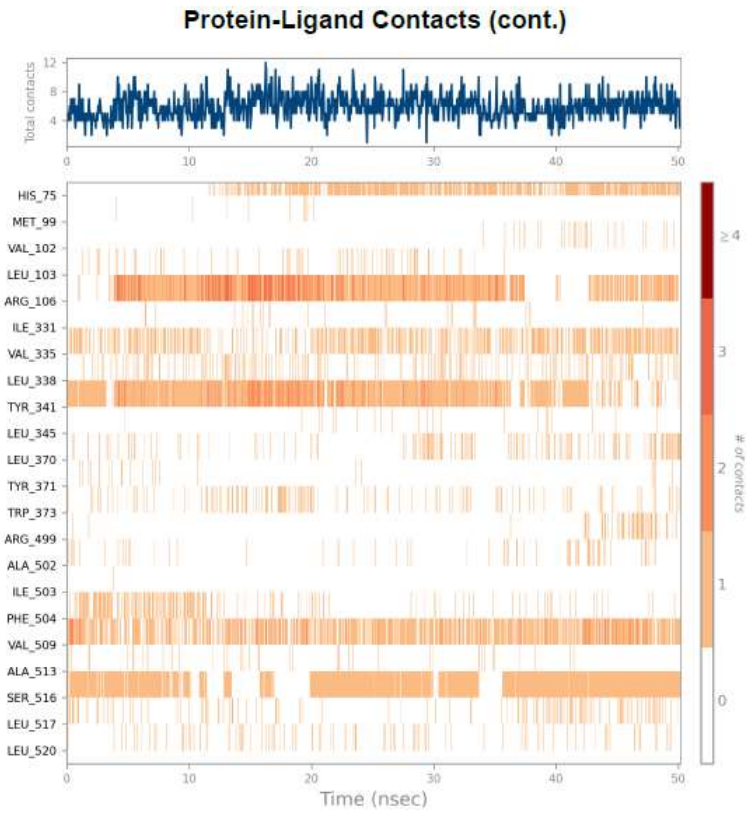

Figure 10: Protein-ligand interactions during Time

The Torsion Profile

The evaluation highlighted the stability of rotatable bonds inside the ligand. The major torsions exhibited restrained conformational pressure, suggesting the ligand adopted an energetically favorable orientation within the active site.

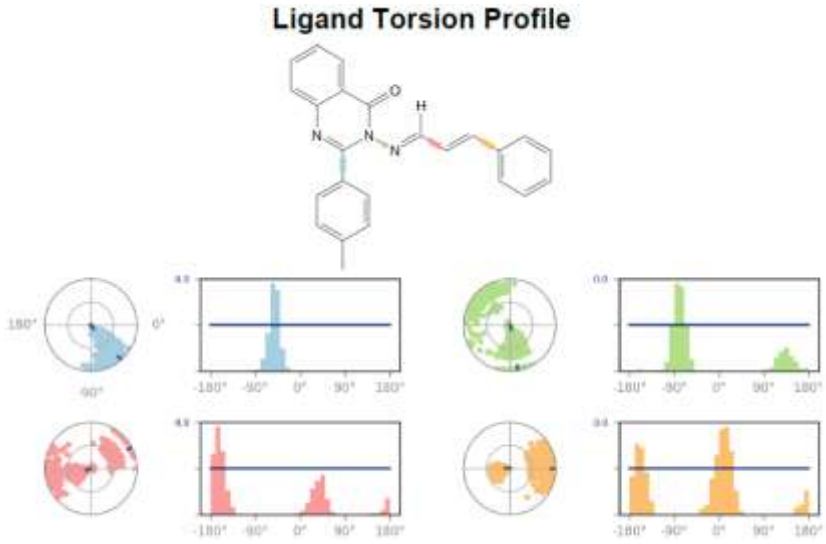

Figure 11: ligand Torsion Profile.

CONCLUSION

The computational study reveals exciting opportunities for establishing new antimicrobial agents by focusing on several crucial bacterial targets. Sophisticated techniques like molecular docking, ADME evaluation, and molecular dynamics simulations were employed to assess both candidate compounds. The docking analysis indicated robust binding of both compounds to the target bacterial and human proteins, with a notable preference for compound 4b over 4a in most bacterial targets, suggesting their potential efficacy in antimicrobial therapy and pain-relieving agents. The ADME evaluation illustrated favorable pharmacokinetic characteristics and limited penetration of the blood-brain barrier. The molecular dynamics simulation demonstrates the stability of the compound and specific binding to the 3LN1 protein, with robust interactions that are critical for antimicrobial activity. The choice of 3LN1 as a target aligns with its essential biological role, making it a valid model for studying potential antimicrobial agents. Further experimental validation and optimization of the compounds are warranted based on these computational insights.

REFERENCES

[1] Yao JD, Moellering Jr RC. Antibacterial agents. Manual of clinical microbiology. 2011:1041-81.
[2] Gould K. Antibiotics: from prehistory to the present day. Journal of Antimicrobial Chemotherapy. 2016;71(3):572-5.
[3] Belete TM. Novel targets to develop new antibacterial agents and novel alternatives to antibacterial agents. Human Microbiome Journal. 2019;11:100052.
[4] Ang JY, Ezike E, Asmar BI. Antibacterial resistance. The Indian Journal of Pediatrics. 2004;71:229-39.
[5] Rice LB, Bonomo RA. Mechanisms of resistance to antibacterial agents. Manual of clinical microbiology. 2011:1082-114.
[6] Halawa EM, Fadel M, Al-Rabia MW, Behairy A, Nouh NA, Abdo M, et al. Antibiotic action and resistance: updated review of mechanisms, spread, influencing factors, and alternative approaches for combating resistance. Frontiers in Pharmacology. 2024;14:1305294.
[7] Li Z, Zhao L, Bian Y, Li Y, Qu J, Song F. The antibacterial activity of quinazoline and quinazolinone hybrids. Current Topics in Medicinal Chemistry. 2022;22(12):1035-44.

[8] Jafari E, Khajouei MR, Hassanzadeh F, Hakimelahi GH, Khodarahmi GA. Quinazolinone and quinazoline derivatives: recent structures with potent antimicrobial and cytotoxic activities. Research in pharmaceutical sciences. 2016;11(1):1-14.
[9] Gatadi S, Lakshmi TV, Nanduri S. 4 (3H)-Quinazolinone derivatives: Promising antibacterial drug leads. European journal of medicinal chemistry. 2019;170:157-72.
[10] Gomaa HA. A comprehensive review of recent advances in the biological activities of quinazolines. Chemical Biology & Drug Design. 2022;100(5):639-55.
[11] Abdulsada AH, Alibeg AAA, Wannas AN. Synthesis and biological evaluation of some newly synthesized Schiff base derived quinazolinone and cinnamaldehyde. Journal of Pharmaceutical Negative Results. 2022;13(3):151-4.
[12] Marufa SS, Rahman T, Rahman MM, Rahman MM, Khan SJ, Jahan R, et al. Design, synthesis, molecular docking, and dynamics studies of novel thiazole-Schiff base derivatives containing a fluorene moiety and the assessment of their antimicrobial and antioxidant activity. RSC advances. 2024;14(47):35198-214.
[13] Haloob A, Faisal M, Raauf AM. In Silico Evaluation of Molecular Docking, Molecular Dynamic, and ADME Study of New Nabumetone Schiff Base Derivatives (1, 3, 4-oxadiazole or 1, 3, 4-thiadiazole ring) Promising Antiproliferation Action Against Lung Cancer. Turkish Computational and Theoretical Chemistry.8(4):114-26.
[14] Eid EE, Azam F, Hassan M, Taban IM, Halim MA. Zerumbone binding to estrogen receptors: An in-silico investigation. Journal of receptors and signal transduction. 2018;38(4):342-51.
[15] Naglah AM, Askar AA, Hassan AS, Khatab TK, Al-Omar MA, Bhat MA. Biological evaluation and molecular docking with in silico physicochemical, pharmacokinetic and toxicity prediction of pyrazolo [1, 5-a] pyrimidines. Molecules. 2020;25(6):1431.
[16] Hassan AS, Morsy NM, Awad HM, Ragab A. Synthesis, molecular docking, and in silico ADME prediction of some fused pyrazolo [1, 5-a] pyrimidine and pyrazole derivatives as potential antimicrobial agents. Journal of the Iranian Chemical Society. 2022;19(2):521-45.
[17] Morris GM, Goodsell DS, Halliday RS, Huey R, Hart WE, Belew RK, et al. Automated docking using a Lamarckian genetic algorithm and an empirical binding free energy function. Journal of computational chemistry. 1998;19(14):1639-62.
[18] Trott O, Olson AJ. AutoDock Vina: improving the speed and accuracy of docking with a new scoring function, efficient optimization, and multithreading. Journal of computational chemistry. 2010;31(2):455-61.
[19] Jones G, Willett P, Glen RC, Leach AR, Taylor R. Development and validation of a genetic algorithm for flexible docking. Journal of molecular biology. 1997;267(3):727-48.
[20] Gad EM, Nafie MS, Eltamany EH, Hammad MS, Barakat A, Boraei AT. Discovery of new apoptosis-inducing agents for breast cancer based on ethyl 2-amino-4, 5, 6, 7-tetra hydrobenzo [b] thiophene-3-carboxylate: Synthesis, in vitro, and in vivo activity evaluation. Molecules. 2020;25(11):2523.
[21] Quintás G, Castell JV, Moreno-Torres M. The assessment of the potential hepatotoxicity of new drugs by in vitro metabolomics. Frontiers in Pharmacology. 2023;14:1155271.
[22] Mulliner D, Schmidt F, Stolte M, Spirkl H-P, Czich A, Amberg A. Computational models for human and animal hepatotoxicity with a global application scope. Chemical Research in Toxicology. 2016;29(5):757-67.
[23] Uesawa Y. Progress in Predicting Ames Test Outcomes from Chemical Structures: An In-Depth Re-Evaluation of Models from the 1st and 2nd Ames/QSAR International Challenge Projects. International Journal of Molecular Sciences. 2024;25(3):1373.
[24] O'Hagan S, Kell DB. The apparent permeabilities of Caco-2 cells to marketed drugs: magnitude, and independence from both biophysical properties and endogenite similarities. PeerJ. 2015;3:e1405.
[25] Cordeiro MM, Salvador A, Moreno MJ. Calculation of Permeability Coefficients from Solute Equilibration Dynamics: An Assessment of Various Methods. Membranes. 2022;12(3):254.
[26] Juvale IIA, Hamid AAA, Abd Halim KB, Has ATC. P-glycoprotein: New insights into structure, physiological function, regulation and alterations in disease. Heliyon. 2022;8(6).
[27] Zhivkova ZD. Quantitative structure–pharmacokinetics relationships for plasma protein binding of basic drugs. Journal of Pharmacy & Pharmaceutical Sciences. 2017;20:349-59.
[28] Watanabe R, Esaki T, Kawashima H, Natsume-Kitatani Y, Nagao C, Ohashi R, et al. Predicting fraction unbound in human plasma from chemical structure: improved accuracy in the low value ranges. Molecular pharmaceutics. 2018;15(11):5302-11.
[29] Smith DA, Beaumont K, Maurer TS, Di L. Volume of distribution in drug design: miniperspective. Journal of medicinal chemistry. 2015;58(15):5691-8.

[30] Gandhi J, Khera L, Gaur N, Paul C and Kaul R (2017) Role of Modulator of Inflammation Cyclooxygenase-2 in Gammaherpesvirus Mediated Tumorigenesis. Front. Microbiol. 8:538.